Journal of Materials Chemistry A

COMMUNICATION

View Article Online
View Journal | View Issue

Cite this: J. Mater. Chem. A, 2017, 5, 11582

Received 27th January 2017
Accepted 10th April 2017

DOI: 10.1039/c7ta00902j

rsc.li/materials-a

Enhanced electrocatalytic performance of palladium nanoparticles with high energy surfaces in formic acid oxidation†

Anna Klinkova,[a] Phil De Luna,[b] Edward H. Sargent,[b] Eugenia Kumacheva[a] and Pavel V. Cherepanov *[c]

Direct formic acid fuel cells hold great potential for utilizing formic acid as an energy source *via* formic acid oxidation (FAO). We report a new anodic material composed of branched Pd nanoparticles (BNPs) with enhanced performance for the electrocatalytic FAO reaction. The results of computational studies indicate that the surface morphology of the nanoparticles favours the binding of FAO intermediates while allowing for field-induced reagent concentration (FIRC) at sharp tips leading to amplified catalytic activity and improved stability. Our findings highlight the importance of morphological control of high-energy surfaces for effective fuel cell anodes.

Direct formic acid fuel cells are promising power sources for portable electronic devices, owing to their high theoretical energy density, as well as safer and easier fuel storage, in comparison with hydrogen fuel cells.[1] In addition, formic acid has a considerably higher energy density and a lower crossover flux through a cation exchange membrane than methanol, thus allowing the utilization of highly concentrated fuel solutions in fuel cells.[2]

Palladium has been recognized as the best anodic monometallic electrocatalyst for the FAO reaction, owing to the high activity of Pd at relatively low potentials.[3] Further optimization of Pd surfaces to maximize the density of active sites is required to achieve the maximum catalytic efficiency at low potentials and to improve the resistance to catalyst poisoning due to the accumulation of CO (a side product) on Pd surfaces.

Two proposed mechanisms of the FAO reaction are as follows:

1. Direct mechanism:

$$HCOOH \rightarrow H^+(aq) + e^- + HCOO^* \quad (1)$$

$$HCOO^* \rightarrow CO_2 + H^+(aq) + e^- \quad (2)$$

2. Indirect mechanism:

$$HCOOH \rightarrow H^+(aq) + e^- + COOH^* \quad (3)$$

$$COOH^* \rightarrow CO^* + OH^* \quad (4)$$

$$CO^* + OH^* \rightarrow CO_2 + H^+ + e^- \quad (5)$$

The direct mechanism, dominant at low applied potentials (~0.4 V RHE), leads to the formation of CO_2 following a two-step proton/electron transfer *via* a HCOO* intermediate (Reactions 1 and 2). The indirect FAO mechanism, prevalent at high applied potentials (>0.6 V RHE), results in the formation of CO *via* a COOH* intermediate (Reactions 3 and 4), which is subsequently oxidized to CO_2 (Reaction 5).[4,5]

The electrocatalytic activity of nanoparticles (NPs) is strongly dependent on their surface morphology, namely their enclosing facets and the presence of under-coordinated surface atoms. Most of the recent reports focus on three surface features in Pd for the FAO reaction: low-index facets,[6,7] lack of well-developed facets (characteristic of small NPs),[8] and twin defects.[4] Among low-index facets, both in the case of electrodes formed from Pd single crystals[6] or Pd NPs enclosed by low index planes of a particular type,[7] the FAO activity increases in the order {110} < {111} < {100}. Recently, it has been found that the introduction of twin defects in Pd NPs enhances their activity in the FAO reaction, in comparison with their single crystal counterparts.[4] Such enhancement was attributed to the lattice strain in the twin boundaries that were indexed to the {211} facets. The DFT calculations showed that the stabilization of intermediates is favoured on the {211} facets, over the {100} and {111} planes.[4] Based on these findings, we hypothesized that Pd NPs with an abundance of high-index planes can be a promising material for further improvement of anode activity (lowering of the onset potential and increasing the current density), as well as stability in the FAO reaction.

[a]Department of Chemistry, University of Toronto, Toronto, Ontario M5S 3H6, Canada
[b]Department of Electrical and Computer Engineering, University of Toronto, Toronto, Ontario M5S 3E4, Canada
[c]Department of Chemical and Biomolecular Engineering, University of Melbourne, Melbourne, VIC 3010, Australia. E-mail: cherepanov.chem@gmail.com

† Electronic supplementary information (ESI) available. See DOI: 10.1039/c7ta00902j

In this regard, it has been shown that for Pt (a metal with a lower catalytic activity towards FAO than Pd), concave and branched Pt NPs exhibit enhanced catalytic activity towards FAO, compared to their low index counterparts.[2] Similarly, sub-micron single-crystal Pd thorns exhibited a higher activity towards FAO than sub-micron Pd particles; however the nature of the active sites and the increase in the catalytic activity of Pd thorns were not discussed.[9] Furthermore, while Pd NPs enclosed by high-index facets had a high catalytic activity in methanol and ethanol electrooxidation,[10] their performance has not been explored in the FAO reaction.

We recently reported that BNPs enclosed by high index facets show superior performance in CO_2 electroreduction to formate and improved stability against CO poisoning, in comparison with Pd NPs with low-index planes.[12] Computational simulations revealed that high-index planes support intermediate binding, which suppresses CO formation and favours the production of formate. Furthermore, BNPs with sharp geometric features are known to concentrate electric fields at the electrode surface, thus enhancing electrocatalysis *via* field-induced reagent concentration.[13] Based on these results, we hypothesized that Pd NPs with high curvature features enclosed by high energy planes are attractive candidates for the electrooxidation of formic acid to CO_2 (that is, the reverse reaction of CO_2 reduction to formate), due to the synergetic effect of reaction intermediate stabilization on high energy planes and field-induced reagent concentration at the high curvature spikes (Fig. 1).

Here we report a theoretical and experimental study of the electrocatalytic performance of Pd BNPs enclosed by high-index planes and under-coordinated surface sites in the FAO reaction. We found that Pd BNPs show a substantially higher catalytic activity and prolonged stability, in comparison with Pd black and Pd nanocubes (NCs) enclosed by {100} facets – the most active in FAO among low-index facets.[6,7]

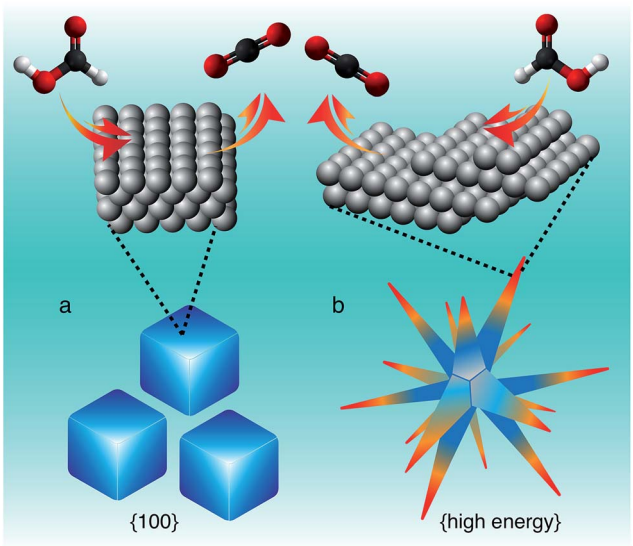

Fig. 1 Schematics showing structural effects responsible for the enhancement of the electrocatalytic performance of metal NPs for (a) cubic and (b) branched structures: facets enclosing NPs favouring intermediate stabilization (top) and sharp features providing high electric fields that induce reagent concentration at the electrode surface (bottom).

In the present work, Pd NCs and BNPs were synthesized by large-scale synthesis in an aqueous suspension of cetyltrimethylammonium bromide.[14,15] Fig. 2 shows the scanning electron microscopy images of the BNPs and NCs. (HRTEM images indicating the presence of high index facets of the BNPs and NCs can be found in the ESI). The side length of the NCs was 48 ± 3 nm, and the size of the BNPs, defined as the diameter of the circle that can fit the BNP, was 110 ± 10 nm. In addition, Pd black (99.95% purity, purchased from Sigma-Aldrich) particles of the size below 20 nm were used as a reference sample. We assume that this reference material has a mixture of low index surfaces with a high proportion of {111} facets as they are the most thermodynamically stable.[16] The NPs were deposited from the NP slurry in the methanol–water mixture onto the carbon paper using Nafion, following an earlier reported protocol.[11] The NPs densely covered a 0.5×0.5 cm area of the carbon paper, with no carbon fibres exposed to the solution. To ensure the removal of cetyltrimethylammonium bromide used as a stabilizer during NP synthesis, the electrodes were excessively washed with methanol.[17]

The electrocatalytic activity of the NPs in the FAO reaction was studied under an Ar atmosphere at a scan rate of 50 mV s^{-1} in a 0.5 M H_2SO_4 solution containing 0.5 M HCOOH. The current density was normalized to the electrochemically active surface area (ECSA) of the electrode, which was determined using a CO stripping method described elsewhere (see ESI† for details).[18] Fig. 3a compares the first cyclic voltammetry (CV) anodic sweeps during FAO for the electrodes coated with either BNPs or NCs. The peaks near 0.1 V are associated with the desorption of under-potentially deposited hydrogen (H_{upd}) from the acidic environment of the electrolyte.[8] With regard to the BNPs, hydrogen desorption started at a lower potential than for the NCs. This trend was in agreement with a lower hydrogen desorption energy of NPs enclosed by high energy surfaces and was attributed to the lower binding energy of hydrogen on the open-structure Pd surfaces than on close-packed atomic structures on low index planes.[17]

The onset potentials for the FAO reaction followed immediately after the H_{upd} atoms desorbed from the electrode surface. In the case of BNPs, FAO had a lower onset potential and a lower anodic peak potential than the NCs or Pd black, providing experimental evidence that a lower energy is required to initiate FAO reaction on the high index planes, compared to the low index planes. In addition, the broadness of the anodic peak of Pd black is indicative of a variety of low index planes,

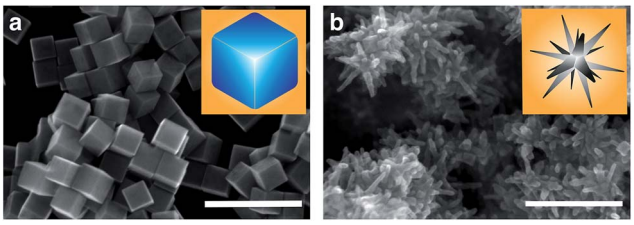

Fig. 2 SEM images of Pd NPs used for electrode fabrication: NCs (a), and BNPs (b). Scale bar 200 nm.

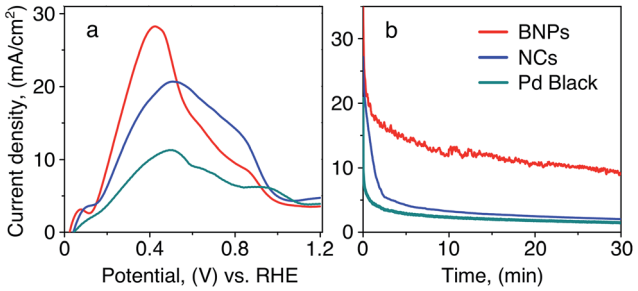

Fig. 3 FAO activity of different Pd NPs and Pd black in Ar-saturated 0.5 M H_2SO_4/0.5 M HCOOH solution: (a) anodic polarization curves at a 50 mV s^{-1} scan rate. (b) Chronoamperometric profiles of BNPs (red), NCs (blue), and Pd black (turquoise) showing ECSA-normalized current densities at +0.15 V.

while the narrow peak at a lower potential for BNPs is in agreement with the presence of highly active sites ascribed to high index facets.

In addition, the ECSA-normalized current density of the BNPs was significantly higher than those of the NCs and Pd black suggesting a faster FAO reaction. This effect was ascribed to the presence of energetically favoured active sites on the BNPs and electric field-induced reagent concentration at the sharp NP features.[13]

Finally, the catalytic stability of BNPs in the FAO reaction was examined and compared to that of the NCs by chronoamperometric measurements at a constant applied potential of 0.4 V *vs.* the RHE. This value of the applied potential is in the region where the direct oxidation pathway (Reactions 1 and 2) is dominant over the indirect oxidation pathway (Reactions 3–5), thereby minimizing CO poisoning.[4] As shown in Fig. 3b, BNPs exhibited a significantly higher ECSA-normalized current density than the NCs and Pd black, and while the current density decayed over time for all NP types, BNPs showed a higher overall stability. More specifically, unlike in the case of BNPs, the major drop in current density for the NCs and Pd black occurred over the course of 150 s, after which the current density remained relatively invariant. Overall, after 30 min of the reaction, the current density was five-fold higher for BNPs than for the NCs (10 *vs.* 2 mA).

DFT calculations were performed to examine the energetics of the direct and indirect pathways of FAO on the {111}, {100}, {110}, and {211} facets (a Pd_{19} cluster was also included in the simulations to illuminate the role of under-coordinated Pd sites). Fig. 4a and b show the reaction energy profile for the direct and indirect oxidation of formic acid at the corresponding dominant potentials of 0.4 V and 0.6 V. Consistent with the results of previous theoretical simulations,[4] we found that the {211} facet exhibited the lowest energies for intermediates of both the direct ($\Delta G_{CHOO^*} = -0.42$ eV) and indirect ($\Delta G_{CO^*+OH^*} = -0.80$ eV) reaction pathways. This finding agreed with our experimental results showing that the Pd BNPs enclosed by high index planes exhibit a higher FAO activity than the {100} facet-enclosed NCs. Interestingly, we found that Pd_{19} clusters that represented under-coordinated sites and adsorbed atoms were more favourable than the NCs for the direct pathway, but less favourable than the NCs

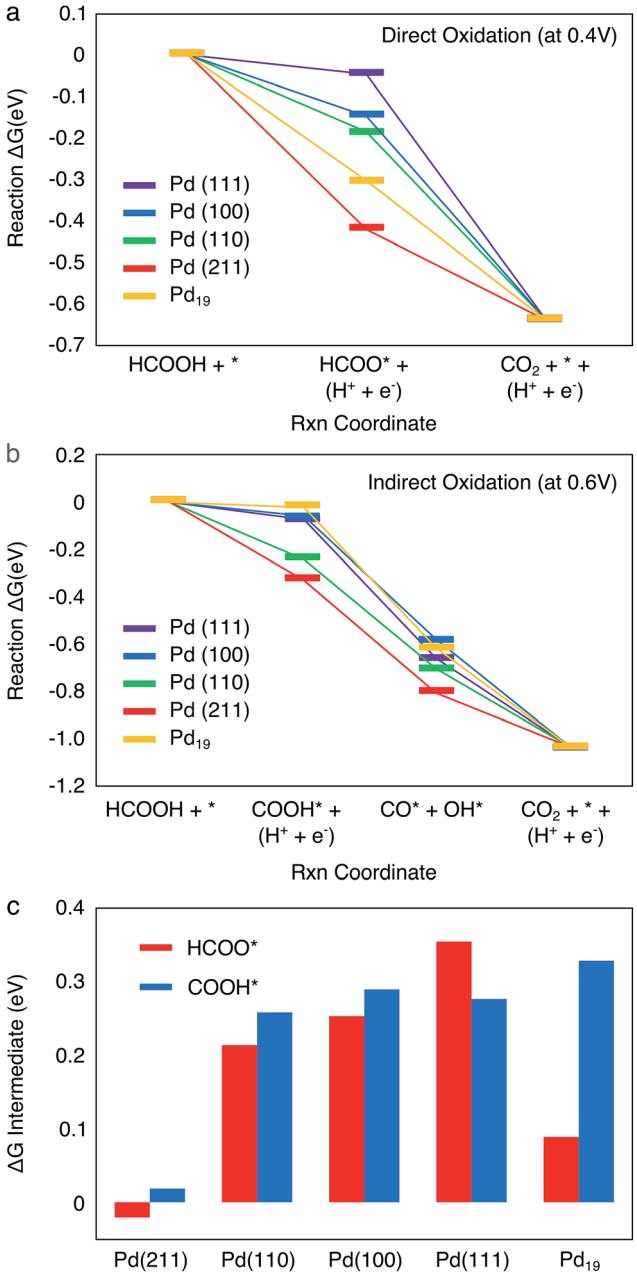

Fig. 4 Reaction energy diagrams for the direct oxidation (a) and indirect oxidation (b) pathways at applied potentials of 0.4 V and 0.6 V respectively on different Pd facets. (c) The $\Delta G_{intermediate}$ for HCOO* and COOH* bound to the different facets.

for the indirect pathway. The indirect pathway leads to the formation of a bound CO* intermediate, which may result in catalyst deactivation due to the CO poisoning. Our results suggest that stepped Pd (211) facets and under-coordinated Pd_{19} clusters favour the direct pathway that is dominant at lower potentials and are less susceptible to CO poisoning. This result explains the higher catalytic stability of BNPs, in comparison with the NCs.

Comparison of the values of the Gibbs free energy of formation of the reaction intermediate, $\Delta G_{intermediate}$, for HCOO* and COOH* on different facets (Fig. 4c) revealed that on

the {211}, {110}, and {100} surfaces, the formation of the HCOO* intermediate was more favoured than that of COOH*, whereas the {111} plane favoured the formation of the COOH* intermediate. The largest difference in the values of $\Delta G_{\text{intermediate}}$ for the HCOO* and COOH* intermediates was for Pd_{19}, that is, the formation of HCOO* was more favoured than that of COOH* by 0.24 eV. Thus, the direct oxidation pathway was the most favourable for the high index planes and adatoms. The indirect oxidation pathway was dominant on the most thermodynamically stable {111} facets that are prevalent in common Pd nano/microscale catalysts (*e.g.*, Pd black[12]).

Interestingly, the DFT calculations suggested that the FAO activity should follow the trend {211} > {110} > {100} > {111}, that is, higher index facets are more catalytically active. This trend was found to hold true in our previous work with CO_2 reduction to formic acid. However, our experimental results, as well as earlier reports,[6,7] show that the {100} facets are more active for FAO than the {110} facets (see ESI†). Further studies are required to address this effect. In contrast to the prevailing idea that catalytic activity correlates linearly with the structural openness of atomic surfaces, more complicated underlying mechanisms of NP performance in FAO have to be investigated.

Conclusions

In summary, we demonstrated that BNPs with high curvature features enclosed by high energy surfaces are a promising type of anodic material for direct formic acid fuel cells, due to their higher electrocatalytic activity and stability in the FAO reaction than Pd NPs with low index facets. Together with earlier studies of the effect of size, shape, and presence of defects in Pd NPs, our findings provide understanding and a basis for the rational design of high performance electrocatalysts for fuel cell applications.

Acknowledgements

A. K., E. H. S., and E. K thank the Connaught Global Challenges Fund of the University of Toronto and the NSERC for the financial support of this work. A. K thanks the Connaught Postdoctoral Fellowship for funding. P. D. L. thanks the NSERC CGS-D for funding. DFT computations were performed using an IBM BlueGene/Q supercomputer at the SciNet HPC Consortium provided through the Southern Ontario Smart Computing Innovation Platform (SOSCIP). P. V. C. thanks the University of Bayreuth and the University of Melbourne for financial support.

Notes and references

1 R. F. Service, *Science*, 2002, **296**, 1222–1224.
2 J. Lai, W. Niu, S. Li, F. Wu, R. Luque and G. Xu, *J. Mater. Chem. A*, 2016, **4**, 807.
3 K. Jiang, H.-X. Zhang, S. Zou and W.-B. Cai, *Phys. Chem. Chem. Phys.*, 2014, **16**, 20360–20376.
4 S. Choi, J. A. Herron, J. Scaranto, H. Huang, Y. Wang, X. Xia, T. Lv, J. Park, H.-C. Peng, M. Mavrikakis and Y. Xia, *ChemCatChem*, 2015, **7**, 2077–2084.
5 R. W. Atkinson, S. S. John, O. Dyck, K. A. Unocic, R. R. Unocic, C. S. Burke, J. W. Cisco, C. A. Rice, T. A. Zawodzinski and A. B. Papandrew, *ACS Catal.*, 2015, **5**, 5154–5163.
6 N. Hoshi, K. Kida, M. Nakamura, M. Nakada and K. Osada, *J. Phys. Chem. B*, 2006, **110**, 12480–12484.
7 X. Zhang, H. Yin, J. Wang, L. Chang, Y. Gao, W. Liu and Z. Tang, *Nanoscale*, 2013, **5**, 8392.
8 M. Shao, J. Odell, M. Humbert, T. Yu and Y. Xia, *J. Phys. Chem. C*, 2013, **117**, 4172–4180.
9 H. Meng, C. Wang, P. K. Shen and G. Wu, *Energy Environ. Sci.*, 2011, **4**, 1522–1526.
10 S. Choi, J. A. Herron, J. Scaranto, H. Huang, Y. Wang, X. Xia, T. Lv, J. Park, H.-C. Peng, M. Mavrikakis and Y. Xia, *ChemCatChem*, 2015, **7**, 2077–2084.
11 N. Tian, Z.-Y. Zhou, N.-F. Yu, L.-Y. Wang and S.-G. Sun, *J. Am. Chem. Soc.*, 2010, **132**, 7580–7581; X. Xie, G. Gao, Z. Pan, T. Wang, X. Meng and L. Cai, *Sci. Rep.*, 2015, **5**, 8515.
12 A. Klinkova, P. De Luna, C.-T. Dinh, O. Voznyy, E. M. Larin, E. Kumacheva and E. H. Sargent, *ACS Catal.*, 2016, **6**, 8115–8120.
13 M. Liu, Y. Pang, B. Zhang, P. De Luna, O. Voznyy, J. Xu, X. Zheng, C. T. Dinh, F. Fan, C. Cao, F. P. G. de Arquer, T. S. Safaei, A. Mepham, A. Klinkova, E. Kumacheva, T. Filleter, D. Sinton, S. O. Kelley and E. H. Sargent, *Nature*, 2016, **537**, 382–386.
14 A. Klinkova, E. M. Larin, E. Prince, E. H. Sargent and E. Kumacheva, *Chem. Mater.*, 2016, **28**, 3196–3202.
15 Y.-H. Chen, H.-H. Hung and M. H. Huang, *J. Am. Chem. Soc.*, 2009, **131**, 9114–9121.
16 H. Ramezani-Dakhel, P. A. Mirau, R. R. Naik, M. R. Knecht and H. Heinz, *Phys. Chem. Chem. Phys.*, 2013, **15**, 5488–5492.
17 A. Klinkova, P. V. Cherepanov, I. G. Ryabinkin, M. Ho, M. Ashokkumar, A. F. Izmaylov, D. V. Andreeva and E. Kumacheva, *Small*, 2016, **18**, 2450–2458.
18 A. S. Baushar and C. A. Rice, *Electrochim. Acta*, 2013, **93**, 152–157.